ARTICLE
Journal of Cellular Biochemistry 111:266–273 (2010)

Journal of Cellular Biochemistry

Novel 14*S*,21-dihydroxy-docosahexaenoic Acid Rescues Wound Healing and Associated Angiogenesis Impaired by Acute Ethanol Intoxication/Exposure

Haibin Tian, Yan Lu, Shraddha P. Shah, and Song Hong*

Louisiana State University, Health Sciences Center, Center of Neuroscience Excellence, New Orleans, Louisiana 70112

ABSTRACT

Acute ethanol intoxication and exposure (AE) has been known to impair wound healing and associated angiogenesis. Here, we found that AE diminished the formation of novel reparative lipid mediator 14*S*,21-dihydroxy-docosa-4*Z*,7*Z*,10*Z*,12*E*,16*Z*,19*Z*-hexaenoic acid (14*S*,21-diHDHA) and its biosynthetic intermediate 14*S*-hydroxy-DHA (14*S*-HDHA) from docosahexaenoic acid (DHA) in murine wounds. However, AE did not reduce the formation of DHA and the intermediate 21-HDHA. These results indicate that in the biosynthetic pathways of 14*S*, 21-diHDHA in wounds, AE suppresses the 14*S*-hydroxy-generating activity of 12-lipoxygenase-like (LOX-like), but does not suppress the 21-hydroxy-generating activity of cytochrome P450 and DHA-generating activities. The AE-suppression of 12-LOX-like activity was further confirmed by the diminished formation of 12-hydroxy-eicosatetraenoic acid in wounds under AE. Supplementing 14*S*,21-diHDHA to wounds rescued the AE-impaired healing and vascularization. 14*S*,21-diHDHA restored AE-impaired processes of angiogenesis *in vitro*: endothelial cell migration, tubulogenesis, and phosphorylation of p38 mitogen-activated protein kinase (MAPK). Taken together, the suppression of 14*S*,21-diHDHA formation is responsible, at least partially, for the AE-impairment of cutaneous wound healing and angiogenesis. Supplementing 14*S*,21-diHDHA to compensate its deficit in AE-impaired wounds rescues the healing and angiogenesis. These results provide a novel mechanistic insight for AE-impaired wound healing that involves the necessary roles of 14*S*,21-diHDHA. They also offer leads for developing 14*S*,21-diHDHA-related therapeutics to ameliorate AE-impairment of wound healing. J. Cell. Biochem. 111: 266–273, 2010.

KEY WORDS: ACUTE ETHANOL INTOXICATION/EXPOSURE; 14*S*,21-DI-HYDROXY-DOCOSAHEXAENOIC ACID; WOUND HEALING; ANGIOGENESIS; VEGF; ENDOTHELIAL CELLS; RE-EPITHELIALIZATION; P38 MAPK

Acute ethanol intoxication and exposure (AE) has been reported to significantly impair wound healing and associated angiogenesis [Radek et al., 2005, 2008; Bird et al., 2009]. Many patients hospitalized for traumatic wounds have AE associated with their injuries [Rivara et al., 1993; Sommers, 1994; Radek et al., 2008]. Angiogenesis or formation of new vessels is paramount for supplying blood for optimal healing [Li et al., 2003; Velazquez, 2007], and this is achieved through the processes including endothelial cell (EC) migration and vascularization. Vascular endothelial growth factor (VEGF) activities in wounds regulate these processes [Brown et al., 1992; Shweiki et al., 1992; Dvorak et al., 1995; Nissen et al., 1998; Ferrara, 2004] and AE impairs VEGF-modulated vascularization [Radek et al., 2005, 2008].

Docosahexaenoic acid (DHA) is an endogenous ω3 essential fatty acid relatively abundant in skin (in full thickness) [Lu et al., 2010]. We have recently revealed the molecular structure of novel endogenous DHA-derived 14*S*,21-di-hydroxy-docosa-4*Z*,7*Z*,10*Z*, 12*E*,16*Z*,19*Z*-hexaenoic acid (14*S*,21-diHDHA) in skin wounds and found that it is a reparative lipid mediator (LM) that promotes wound healing [Lu et al., 2010]. It has been known that AE dysregulates the biosynthesis of LMs [Shukla et al., 2001; Molina, 2008; Sozio and Crabb, 2008]. However, there are no reports regarding the roles of LMs in AE-impaired wound healing and angiogenesis, no mention of 14*S*,21-diHDHA.

Here, we found that in skin wounds of mice, AE suppressed the formation of 14*S*,21-diHDHA and its biosynthetic intermediate 14*S*-hydroxy-DHA (14*S*-HDHA), which indicates that AE suppresses the 14*S*-hydroxy-generating activity of 12-lipoxygenase-like (12-LOX-like) for the biosynthesis of 14*S*,21-diHDHA in wounds. However, AE did not reduce the formation of 21-HDHA (another

Additional Supporting Information may be found in the online version of this article.

NIH fund 1R01DK087800 (to S.H.); startup fund (to S.H.) from Center of Neuroscience Excellence, LSUHSC-New Orleans; and Bridge and Supplemental Grant 2009 (To S.H.) from LSUHSC-New Orleans.

*Correspondence to: Song Hong, LSUHSC—Center of Neuroscience Excellence, Lions Building, 2020 Gravier St., Suite D, New Orleans, LA 70112. E-mail: shong@lsuhsc.edu

Received 1 April 2010; Accepted 11 May 2010 • DOI 10.1002/jcb.22709 • © 2010 Wiley-Liss, Inc.
Published online 19 May 2010 in Wiley Online Library (wileyonlinelibrary.com).

intermediate) and DHA (the precursor), suggesting that AE does not suppress the 21-hydroxy-generating activity of cytochrome P450 and DHA-generating activity of lipases for the biosynthesis. Furthermore, applying 14*S*,21-diHDHA to wounds of mice rescued AE-impaired healing and associated proliferative-phase angiogenesis. We also found that 14*S*,21-diHDHA counteracts AE-impairment of EC migration and vasculature formation. These results provide novel leads for developing therapeutics useful for restoring AE-impaired wound healing.

MATERIALS AND METHODS

SPLINTED EXCISIONAL-WOUND HEALING MODEL

Published procedures were followed [Galiano et al., 2004a, b; Radek et al., 2005] with minor modifications. Briefly, PBS (sterile) with or without ethanol (20%) were injected into each mouse (150 μl, i.p., C57BL/6J, female, 8–10 weeks old, 17–21 g; Jackson Laboratory, Bar Harbor, ME). After 30 min, the ethanol-treated mice had a blood ethanol of ~100 mg/dl, just above the legal limit in most states [Radek et al., 2005]. After 24 h the blood ethanol was undetectable [Radek et al., 2005]. Under sterile conditions, paired 4-mm circular, full-thickness wounds were made symmetrically along the midline on the dorsal skin of the anesthetized mice with and without AE. For each wound, PBS or PBS with 14*S*,21-diHDHA (50 ng) was applied to the wound-bed (10 μl) and injected intradermally to four points (10 μl/site) evenly distributed near the wound edge (50 μl total). A donut-shaped 0.5 mm-thick silicone splint (Grace Bio-Laboratories, Bend, OR) was adhered to the skin and the wounds were centered within the splint [Galiano et al., 2004a,b]. The splints prevent murine skin contraction to allow wounds to heal through granulation and re-epithelialization, which closely parallels human wound healing [Galiano et al., 2004a,b].

Histological analysis of wound healing. The established procedures were followed [Galiano et al., 2004a,b; Radek et al., 2005; Wu et al., 2007]. Briefly, wounds with 2 mm normal skin rims were excised from mice sacrificed at days 5 and 7 postwounding [Galiano et al., 2004a,b], fixed in 4% paraformaldehyde, and then embedded in OCT (Tissue-Tec, Torrance, CA). Cryosections (10 μm thick/section) of wounds at day 5 postwounding were analyzed to determine the relative epithelial gap (% of initial wounds) and granulation tissue area after hematoxylin and eosin (H & E) staining. Wound vascularity (vessel density) at day 7 postwounding was assessed [Radek et al., 2005]. Cryosections were pretreated with 0.3% hydrogen peroxide for 15 min at room temperature to block endogenous peroxidase activity, and then blocked in PBS containing 1% fetal bovine serum for 1 h. Cryosections were stained with primary antibody, rat anti-mouse CD31 (BD Biosciences, San Jose, CA), and then with anti-rat Ig horseradish peroxidase (HRP) detection kits (BD Biosciences). Nuclei were stained with hematoxylin. The images were recorded by Nikon TS-100 microscope with a CCD color camera (Nikon, Tokyo, Japan). Three fields in wound-bed were analyzed for each cryosection. The CD31-positive area per field within the wound bed was assessed by NIH Image J1.40 software and averaged for each wound, and the percent vascularity was calculated as (CD31-positive area per field/total wound bed area per field) × 100%.

SAMPLE PREPARATION AND ANALYSIS OF LIPID MEDIATORS

Prostaglandin $F_{2\alpha}$-d_4 ($PGF_{2\alpha}$-d_4), DHA, and Leukocyte-12-LOX (L-12-LOX) were purchased from Cayman (Ann Arbor, MI). Wounded-skin was collected from mice immediately following sacrifice at day 1 postwounding. Tissues were submerged in acetone containing $PGF_{2\alpha}$-d_4 as an internal standard (20 ng/sample; 4°C). The samples were extracted with acetone and extracts were purified via C18-solid-phase extraction, and then analyzed via LC–MS/MS (LTQ; Thermo, Waltham, MA) equipped with a chiral column (AD-RH, 150 mm × 2.1 mm × 5 μm; Chiral Tech., West Chester, PA) [Schneider et al., 2007]. The mobile phase had a flow-rate of 0.15 ml/min, eluted as D (acetonitrile:H_2O:acetic acid = 45:55:0.01) from 0 to 45 min, ramped to acetonitrile from 45.1 to 60 min, flowed as acetonitrile for 10 min, and then run as D again for 10 min. Conditions for mass spectrometry were: electrospray, 4.2 kV; heating capillary, −45 V and 290°C; tube lens offset, 70 V; and sheath N_2 gas, 1.2 L/min; and helium gas, 0.1 Pa as a collision gas. The collision energy was between 20% and 35%. A relative collision-energy of 0% to 100% corresponds to a high frequency alternating voltage for resonance excitation from 0 to 5 V maximum. The raw data of LC–MS or MS/MS were acquired in full-scan modes (m/z 100–500 for MS and MS/MS) and used for structure identification and quantification of lipids [Lu et al., 2007]. The quantification is based on the peak areas of LC–MS/MS or LC–MS extracted ion chromatograms of the identified compounds [Bazan et al., 2008].

14*S*,21-diHDHA preparation. LM 14*S*,21-diHDHA was prepared by incubating 14*S*-hydroxy-DHA (14*S*-HDHA; 50 μg) with human P450 (BioCatalytics, Pasadena, CA). 14*S*-HDHA was prepared by incubating DHA (50 μg) with porcine L-12-LOX (1,000 unit; Cayman) in Tris buffer (pH 7.4, with 0.01% X-114 Triton, 37°C, 20 min). The incubations were extracted with two volumes of ethyl acetate three times. The extracts were reconstituted into methanol. 14*S*,21-diHDHA or 14*S*-HDHA in final solutions was separated and quantified by the LC–MS/MS as above [Hong et al., 2003, 2007].

PROCESSES OF ANGIOGENESIS: MIGRATION AND VASCULATURE FORMATION

Isolation and identification of murine microvascular endothelial cells (mMVECs). This was done as described previously [Cha et al., 2005] and as detailed in Supplemental materials. The final mMVECs were 95% CD31+ and VE-cadherin+.

mMVEC migration. Cell migration was performed as described previously [Bajpai et al., 2007]. Cell culture inserts containing membranes with 8 μm pore size were placed in a 24-well tissue culture plate (BD Biosciences). The underside of the membrane was coated with 0.5% gelatin at 4°C overnight and then blocked with 0.1% BSA at 37°C for 1 h. Quiescenced mMVECs were prepared by starvation in DMEM containing 0.5% FBS with or without AE (100 mg/dl ethanol) for 24 h, then suspended in 100 μl DMEM in the upper chamber of a 24-transwell plate (1×10^5 cells/well). The lower chamber was added with 800 μl DMEM containing AE, 14*S*,21-diHDHA, murine VEGF isoform 164 (mVEGF164; Invitrogen), mVEGF164 + AE, or mVEGF164 + AE + 14*S*,21-diHDHA, where AE was 100 mg/dl, 14*S*,21-diHDHA was 100 nM, and mVEGF164 was

50 ng/ml. DMEM alone was used as non-AE control. Transmigration was carried out for 4 h (37°C, 5% CO_2). Migrated cells on the underside of the membrane were stained with Giemsa, and then counted in five randomly selected fields/well using a microscope. Results were expressed as migrated cells/field.

mMVEC tubulogenesis. The *in vitro* tubulogenesis parallels the *in vivo* vasculature formation. Published procedures were followed with minor modifications [Radek et al., 2005, 2008]. Briefly, quiescenced mMVECs (2×10^4) adhered to prepared Matrigel in a 96-well culture plate were cultured (37°C, 5% CO_2, 6 h) in DMEM containing AE, 14*S*,21-diHDHA, mVEGF164, mVEGF164 + AE, or mVEGF164 + AE + 14*S*,21-diHDHA, where AE was 100 mg/dl, 14*S*,21-diHDHA was 100 nM, and mVEGF164 was 50 ng/ml. DMEM alone was used as the non-AE control. In another experiment, mMVECs on prepared Matrigel were cultured in DMEM containing 0–1,000 nM 14*S*,21-diHDHA under AE (100 mg/dl) and non-AE. The tubular length was measured using a microscope and NIH Image J1.40 software. Tubular length of each group was normalized to the value of non-AE control.

Western blot. This was performed according to published specifications [Siebert et al., 2001]. Briefly, quiescent mMVECs were incubated in DMEM containing AE, 14*S*,21-diHDHA, mVEGF164, 14*S*,21-diHDHA + AE, mVEGF164 + AE, mVEGF164 + 14*S*,21-diHDHA, or mVEGF164 + AE + 14*S*,21-diHDHA for 30 min, where AE was 100 mg/dl, 14*S*,21-diHDHA was 100 nM, and mVEGF164 was 50 ng/ml. DMEM alone was used as the non-AE control. Cells were lyzed for the analysis of expression of P-p38 (phosphorylated form of p38) and p38 (non-phosphorylated form). Total protein (30 μg) of each sample was separated by electrophoresis on a 10% polyacrylamide gel, transferred onto a polyvinylidene fluoride membrane (Millipore, Billerica, MA), and then stained with specific antibodies: P-p38 as well as p38 (BD biosciences). The images was analyzed using Odyssey Imaging System (LI-COR, Lincoln, NE) [Tian et al., 2009].

RESULTS

THE FORMATION OF 14*S*,21-diHDHA WAS REDUCED IN WOUNDS UNDER AE

14*S*,21-diHDHA was identified in wounds of non-AE control C57BL/6J mice (Fig. 1A), and its formation was diminished in wounds of mice under AE (Fig. 1A left inset, right panel) based on the LC–MS/MS analysis. 14*S*,21-diHDHA structure (Fig. 1A right inset) is revealed by its LC–MS/MS ions at mass to charge ratios (*m*/*z*) 359 $[M-H]^-$, 323 $[M\text{-}H\text{-}2H_2O]^-$, 315, 279 $[M\text{-}H\text{-}CO_2\text{-}2H_2O]^-$, 271 $[315\text{-}CO_2]^-$, 253 $[315\text{-}CO_2\text{-}H_2O]^-$, 233, 205, 161 $[205\text{-}CO_2]^-$, and 215 $[233\text{-}H_2O]^-$ (Fig. 1A); as well as its LC retention time (RT); both matched those of 14*S*,21-diHDHA generated from DHA by

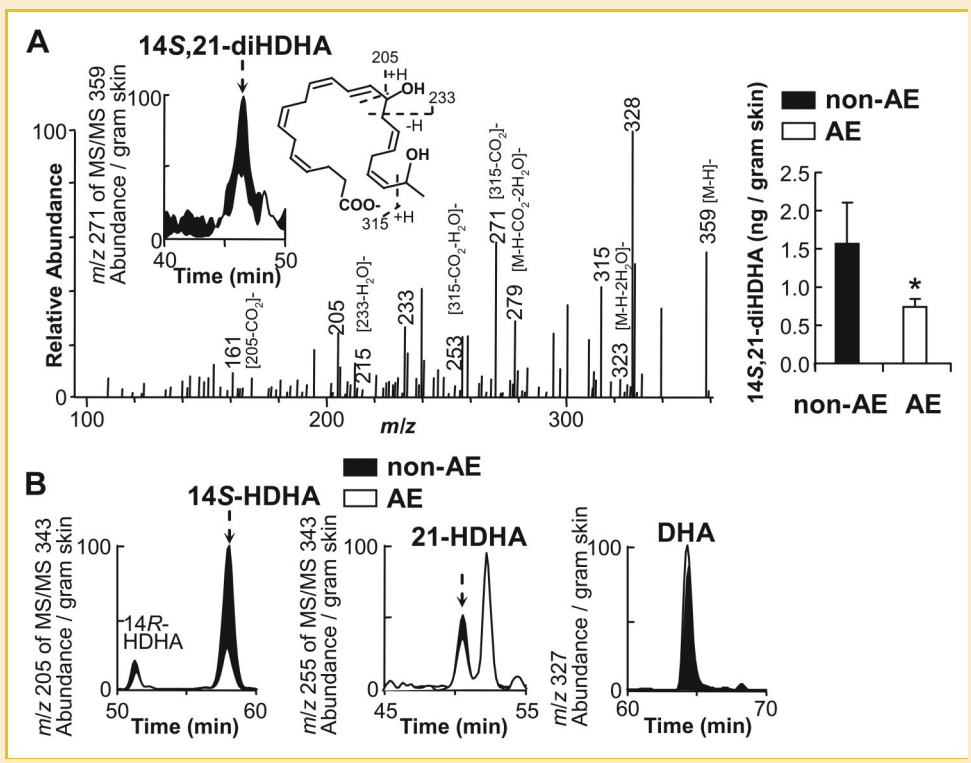

Fig. 1. AE reduced the formation of novel 14*S*,21-diHDHA and its biosynthetic intermediate 14*S*-HDHA in skin wounds. Splinted-excisional-wounds were made to C57BL/6J mice that underwent AE or non-AE control (PBS alone). Wounded skin was collected from mice at day 1 postwounding (n = 6), then analyzed as detailed in Materials and Methods Section. A: The LC–MS/MS spectrum (left), chromatogram (left inset), structure elucidation (middle inset), and quantification (right) of 14*S*,21-diHDHA from wounds. B: LC–MS/MS chromatograms of 14*S*-HDHA (left), 21-HDHA (middle), and DHA (right) from wounds. For comparison, the ion abundance of each MS/MS chromatogram was divided by the extraction recovery of internal standard spiked to the sample, and then normalized for per gram of skin. Results are expressed as mean ± SEM. $^*P < 0.05$ for the comparison between AE and non-AE control.

sequential catalysis of L-12-LOX and P450 [Lu et al., 2010]. The LC peak area of 14*S*,21-diHDHA under AE is smaller than that under non-AE (Fig. 1A left inset). Additionally, from wounds, we found 14*S*-HDHA, 21-HDHA, and DHA, the procusors for the 14*S*,21-diHDHA biosynthesis [Lu et al., 2010], whose LC–MS/MS spectra and RTs matched those published before (Fig. 1B) [Lu et al., 2010]. The LC peak area of 14*S*-HDHA in wounds with AE was much less than that without AE (Fig. 1B left), while the peak areas for 21-HDHA (Fig. 1B middle) and DHA (Fig. 1B right) were near the same, which indicates that AE reduced the formation of 14*S*-HDHA in wounds, but did not affect the formation of 21-HDHA and DHA.

14*S*,21-diHDHA RESCUED AE-IMPAIRED WOUND HEALING

Because AE impairs wound healing [Radek et al., 2005] and 14*S*,21-diHDHA formation (Fig. 1), we tested whether applying 14*S*,21-diHDHA to wounds could reduce AE-impairment of the healing. Compared to wounds of non-AE control, wounds under AE had larger relative epithelial gap ($77.6 \pm 4.0\%$ for AE control vs $53.9 \pm 3.5\%$ for non-AE control) and less granulation tissue formation (4493.3 ± 520.6 for AE control vs 8599.0 ± 552.9 pixels/section for non-AE control) at day 5 postwounding based on the analysis of cryosections with H & E staining (Fig. 2A–C). However, 14*S*,21-diHDHA treatment of wounds under AE significantly promoted would healing compared to AE control: it accelerated re-epithelialization for having smaller relative epithelial gap ($59.0 \pm 2.9\%$; Fig. 2A,B), and increased granulation tissue area (7272.5 ± 373.2 pixels/section; Fig. 2A,C). In addition, 14*S*,21-diHDHA treatment of wounds without AE had smaller epithelial gap and more granulation tissue compared to non-AE control (Fig. 2A–C). The relative epithelial gap and granulation tissue area of 14*S*,21-diHDHA-treated wounds under AE were not significantly different with those of non-AE control, which indicates that 14*S*,21-diHDHA rescues AE-impaired wound healing (Fig. 2A–C).

14*S*,21-diHDHA RECOVERED VASCULARIZATION/ANGIOGENESIS IN AE-IMPAIRED WOUNDS

Considering that angiogenesis in wound healing is critical [Li et al., 2003; Velazquez, 2007] and impeded by AE [Radek et al., 2005, 2008], we studied whether 14*S*,21-diHDHA recovers AE-impaired angiogenesis during wound healing. 14*S*,21-diHDHA under non-AE significantly promoted angiogenesis by increased wound vascularity ($15.2 \pm 0.7\%$) compared to non-AE control ($11.0 \pm 0.9\%$; Fig. 2D,E). Wounds under AE exhibited decreased wound vascularity ($5.1 \pm 0.5\%$) compared to non-AE control, which is consistent with a previous report [Radek et al., 2005]. However, when 14*S*,21-diHDHA was injected into wounds under AE, the wound vascularity ($12.5 \pm 0.9\%$) was significantly increased compared to that of wounds from AE treatment. Therefore, 14*S*,21-diHDHA recovered the angiogenesis in wounds.

14*S*,21-diHDHA RESCUED AE-IMPAIRED PROCESSES OF ANGIOGENESIS

We questioned whether 14*S*,21-diHDHA could modulate the processes of angiogenesis, EC migration, and vasculature formation. Without mVEGF164 stimulation, AE treatment had no effect on mMVEC migration compared to non-AE control (DMEM without ethanol) (74.8 ± 2.5 cells/field for AE treatment vs 73.6 ± 3.9 cells/field for non-AE control, Fig. 3A,B). 14*S*,21-diHDHA significantly promoted mMVEC migration (105.8 ± 5.6 cells/field) when mVEGF164 and AE were absent. AE (100 mg ethanol/dl) significantly inhibited mVEGF164-induced mMVEC migration (95.4 ± 5.5 for [AE + mVEGF164] vs 152.4 ± 4.7 cells/field for mVEGF164 alone). 14*S*,21-diHDHA significantly increased the AE-impaired VEGF-modulated mMVEC migration (140.5 ± 5.0 cells/field; Fig. 3A,B).

The tubulogenesis for AE alone is not significantly different from that in non-AE control. However, under mVEGF164 stimulation, AE significantly decreased the tubular length compared to mVEGF164 alone, which is consistent with previous report [Radek et al., 2005, 2008]. This impairment was rescued by 14*S*,21-diHDHA treatment that increased the AE-impaired and VEGF-regulated tubulogenesis of mMVECs. It is observed that 14*S*,21-diHDHA alone also promoted tubulogenesis without the addition of VEGF (Fig. 3C,D). In addition, 14*S*,21-diHDHA enhanced the effect of mVEGF164 on EC migration and tubulogenesis (Fig. 3A–D). Higher concentration of 14*S*,21-diHDHA resulted in larger mMVEC tubular lengths, that is, more tubulogenesis, except that the difference on tubulogenesis is small for 100 and 1,000 nM or for 0 and 1 nM (Fig. 3E). AE reduced the enhancement by14*S*,21-diHDHA (10, 100, or 1,000 nM) on mMVEC tubulogenesis. However, AE did not affect the response to 0 or 1 nM 14*S*,21-diHDHA (Fig. 3E). Taken together 14*S*,21-diHDHA is able to rescue the AE-impaired cellular processes of angiogenesis by significantly increasing mMVEC tubulogenesis and migration.

14*S*,21-diHDHA RECOVERED AE-IMPAIRED P38 PHOSPHORYLATION

Activation of MAPK pathways is essential in wound healing and associated angiogenesis [Sharma et al., 2003; Bajpai et al., 2007; Gee et al., 2010]. Since AE impairs VEGF-induced EC migration and vasculature formation as well as 14*S*,21-diHDHA rescues AE-impaired processes of angiogenesis (Fig. 3), we postulated that 14*S*,21-diHDHA could recover AE-impaired phosphorylation signalings. 14*S*,21-diHDHA directly triggered p38 phosphorylation under AE and non-AE (Fig. 3F,G). Although AE alone had no effect on p38 phosphorylation in mMVECs compared to non-AE control, it significantly decreased the levels of the phosphorylated-p38 induced by mVEGF164 or 14*S*,21-diHDHA (Fig. 3F,G). 14*S*,21-diHDHA recovered AE-impaired p38 phosphorylation induced by mVEGF164 in mMVECs. However, AE did not significantly affect p38 phosphorylation in mMVECs modulated by mVEGF164 and 14*S*,21-diHDHA together (see last two bars in Fig. 3G), which further indicates that 14*S*,21-diHDHA meliorate the AE impairment of VEGF-modulated p38 phosphorylation (see last four bars in Fig. 3G). Furthermore, our studies indicate that 14*S*,21-diHDHA did not affect the phosphorylation of VEGF receptor 2 (data not shown).

DISCUSSION

AE impeded the formation of 14*S*,21-diHDHA and 14*S*-HDHA in wounds (Fig. 1), which correlated with AE-impaired healing and angiogenesis (Figs. 2 and 3). 14*S*-HDHA is generated from DHA by

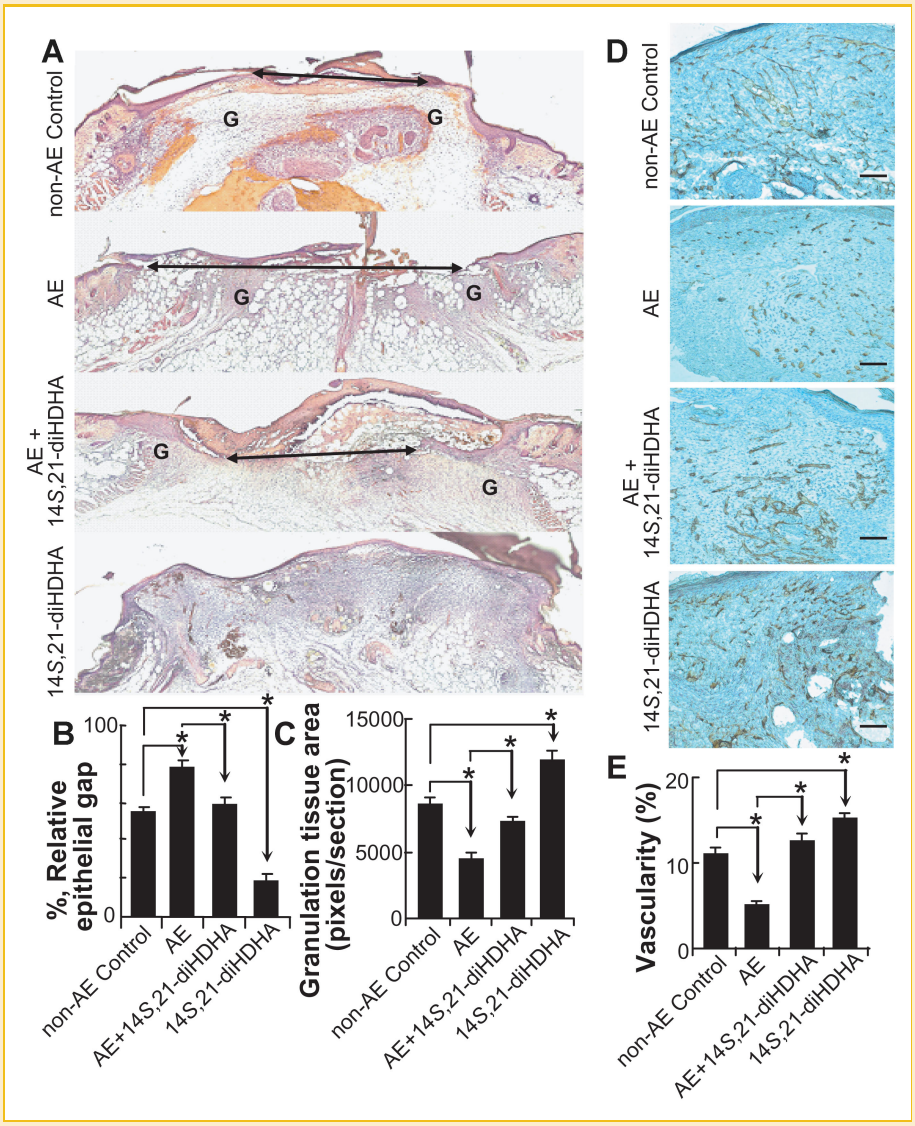

Fig. 2. Supplementing 14*S*,21-diHDHA rescued AE-impaired wound healing and associated vascularization or angiogenesis. The experiments of AE and wounding were conducted as those in Figure 1. A: Micrographs and quantitative analysis of H & E stained cryosections of wounds, collected at day 5 postwounding, show that supplementing 14*S*,21-diHDHA rescued AE-impaired B: re-epithelialization and C: granulation tissue formation by reducing epithelial gap and increasing the total granulation tissue area ($n = 6$, G = granulation tissue, Double arrow = epithelial gap); D: Microphotographs and (E) the quantitative analysis of wound vascularity (%) as (CD31-positive area per field/total wound bed area per field) × 100 at day 7 postwounding show that 14*S*,21-diHDHA rescued vascularization in wounds by increasing vascularity ($n = 12$, original magnification: 100×, scale bar represents 100 μm). Results were mean ± SEM with $^{*}P < 0.05$ for the comparisons marked in the graphs.

12-LOX-like in wounds or blood cells including platelets and macrophages [Kim et al., 1990; Lu et al., 2010], and then transformed by P450 to 14*S*,21-diHDHA [Lu et al., 2010]. 21-HDHA was generated from DHA by P450 activity in tissues and blood cells [VanRollins et al., 1984; Lu et al., 2010] and subsequently converted to 14*S*,21-diHDHA by 12-LOX-like (Fig. 1) [Lu et al., 2010]. DHA mainly results from the hydrolysis of esterified DHA by lipases [Bazan, 2007]. The tentative biosynthetic pathways for 14*S*,21-diHDHA from DHA in wounds are summarized (Scheme 1), where AE suppresses the 14*S*-hydroxy-generating activity of 12-LOX-like in wounds but does not suppress the 21-hydroxy-generating activity of cytochrome P450 and DHA-releasing activity of lipases. Consistent with these findings, in wounds AE suppressed the formation of 12*S*-hydroxy eicosatetraenoic acid, the marker of 12-LOX-like activity [Funk et al., 2002], but did not decrease the generation of unesterified arachidonic acid (Supplemental Fig. 1). L-12-LOX was used here for the enzymatic synthesis of 14*S*-HDHA and 14*S*,21-diHDHA. AE is known to greatly reduces leukocyte infiltration to wounds or inflammation sites as well as leukocyte activation [Radek et al., 2009], which may significantly contribute to the reduction of 14*S*-hydroxy-generating L-12-LOX-like activity. P-12-LOX also has the14*S*-hydroxy-generating activity [Kim et al., 1990]. AE could also affect the 14*S*-hydroxy-generating activity of Platelet-12-LOX. Further

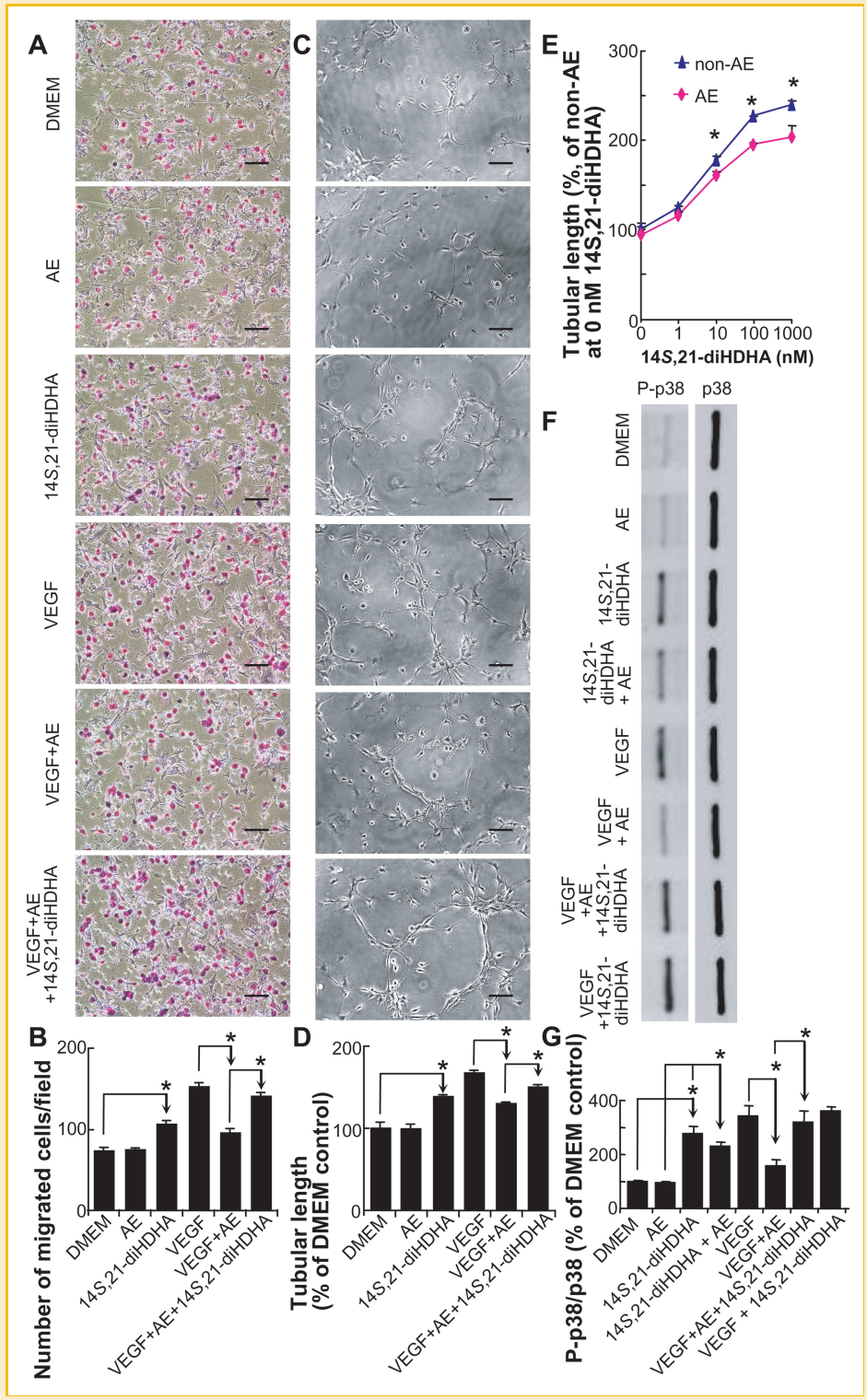

Fig. 3. 14*S*,21-diHDHA promoted the AE-impaired processes of wound healing-associated angiogenesis: mMVEC migration, tubulogenesis, and p38 MAPK phosphorylation. A: Micrographs of migrated mMVECs. B: Number of migrated mMVECs/field ($n = 10$). C: Representative images of mMVEC tube structures. D: The quantification of mMVEC tubular lengths (% of non-AE control). E: mMVEC tubular lengths (% of non-AE control) for treatment with different concentrations (0–1,000 nM) of 14*S*,21-diHDHA under AE (100 mg/dl) or non-AE (DMEM). F: Western blot images and G: relative amounts of phospho-p38 and p38 MAPK in mMVECs show that 14*S*,21-diHDHA triggered p38 phosphorylation and counteracted the AE impairment on this signaling activation. For (C) to (G), $n = 3$. The lower chambers in (A,B), culture-wells for tubulogenesis in (C), or culture-wells for p38 MAPK phosphorylation in (F,G) was added with DMEM containing AE, 14*S*,21-diHDHA, 14*S*,21-diHDHA + AE, mVEGF164, mVEGF164 + AE, mVEGF164 + AE + 14*S*,21-diHDHA, or mVEGF164 + 14*S*,21-diHDHA, where AE was 100 mg/dl, 14*S*,21-diHDHA was 100 nM, and mVEGF164 was 50 ng/ml. DMEM alone was used as non-AE control. Original magnification: 100×, scale bar represents 100 μm. Results were mean ± SEM. $^*P < 0.05$ for the marked comparisons.

studies will be required. Nonetheless epidermis-12-LOX and 12*R*-LOX are likely to be inefficient in the transformation of DHA [Siebert et al., 2001].

Applying 14*S*,21-diHDHA to AE-impaired wounds to compensate the 14*S*,21-diHDHA deficit (Fig 1A) restored the normal re-epithelialization and granulation tissue formation (Fig. 2), which defines the role of 14*S*,21-diHDHA for rescuing wound healing (Fig. 2). Re-epithelialization is one of the main processes of wound healing. It provides the basis for subsequent processes, such as fibroblast proliferation and migration, and granulation tissue formation [Braiman-Wiksman et al., 2007]. AE-impairment of healing that we observed in a splinted-wound model is consistent with those observed using a non-splinted-wound model [Radek et al., 2005].

We also found that 14*S*,21-diHDHA restores AE-impaired wound vascularization or angiogenesis *in vivo* (Fig. 2). 14*S*,21-diHDHA by itself enhances EC tubulogenesis and migration *in vitro*. More interestingly it can rescue AE-impaired VEGF-mediated EC tubulogenesis and migration (Fig. 3, Scheme 1), as well as promote such EC tubulogenesis in a dose-dependent manner (Fig. 3E). 14*S*,21-diHDHA recovers AE-impaired phosphorylation of p38 induced by VEGF [Radek et al., 2008] (Fig. 3F,G), which confirms that it promotes AE-impaired angiogenesis by altering EC response to angiogenic signals. More signaling transduction mechanisms for the action of 14*S*,21-diHDHA are of our interest for future study. Our new finding that AE inhibits VEGF-regulated mMVEC migration parallels AE-impairment to wound angiogenesis because EC migration is a pivotal step of angiogenesis; 14*S*,21-diHDHA not only promotes EC migration, more importantly it restores AE-impaired VEGF-regulated EC migration (Fig. 3A,B). In conclusion (Scheme 1), AE suppresses the formation of 14*S*,21-diHDHA in wounds. Supplementing 14*S*,21-diHDHA to compensate its deficit in wounds rescues the AE-impaired healing and vascularization; 14*S*,21-diHDHA also restores the AE-impaired cellular processes of angiogenesis and p38 MAPK phosphorylation signaling. Our studies provide a mechanistic insight to the rescue of healing and angiogenesis of AE-impaired wounds by the endogenous reparative LM 14*S*,21-diHDHA.

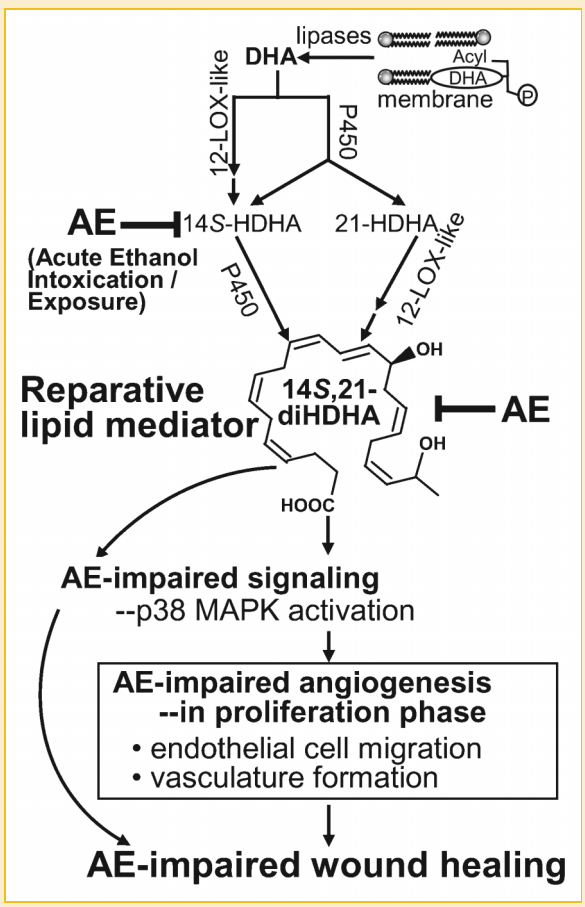

Scheme. 1. A mechanistic diagram for the impairment of cutaneous wound healing by acute ethanol intoxication and exposure: AE-di-minished formation of reparative lipid mediator 14*S*,21-diHDHA in wounds contributes to AE-impairment of healing and associated vascularization/angiogenesis. AE suppresses the generation of 14*S*,21-diHDHA in wounds by decreasing 14*S*-hydroxy-generating 12-LOX-like activity. Supplementing 14*S*,21-diHDHA rescues AE-impaired wound healing and angiogenesis.

ACKNOWLEDGMENTS

We thank Mr. Ryan R. Labadens for his expertise in editing and manuscript preparation. This work is sponsored by NIH fund 1R01DK087800 (to S.H.); startup fund (to S.H.) from Center of Neuroscience Excellence, LSUHSC-New Orleans; and Bridge and Supplemental Grant 2009 (To S.H.) from LSUHSC-New Orleans.

REFERENCES

Bajpai AK, Blaskova E, Pakala SB, Zhao T, Glasgow WC, Penn JS, Johnson DA, Rao GN. 2007. 15(S)-HETE production in human retinal microvascular endothelial cells by hypoxia: Novel role for MEK1 in 15(S)-HETE induced angiogenesis. Invest Ophthalmol Vis Sci 48:4930–4938.

Bazan NG. 2007. Homeostatic regulation of photoreceptor cell integrity: Significance of the potent mediator neuroprotectin D1 biosynthesized from docosahexaenoic acid: The Proctor Lecture. Invest Ophthalmol Vis Sci 48:4866–4881, biography 4864–4865.

Bazan NG, Marcheselli VL, Lu Y, Hong S, Jackson F. 2008. Lipidomic approaches to neuroprotection signaling in the retinal pigment epithelium. In Fliesler SJ, Kisselev OG, editors. Signal Transduction in the Retina. Boca Raton, FL: CRC Press.

Bird MD, Choudhry MA, Molina PE, Kovacs EJ. 2009. Alcohol and trauma: A summary of the Satellite Symposium at the 30th Annual Meeting of the Shock Society. Alcohol 43:247–252.

Braiman-Wiksman L, Solomonik I, Spira R, Tennenbaum T. 2007. Novel insights into wound healing sequence of events. Toxicol Pathol 35:767–779.

Brown LF, Yeo KT, Berse B, Yeo TK, Senger DR, Dvorak HF, van de Water L. 1992. Expression of vascular permeability factor (vascular endothelial growth factor) by epidermal keratinocytes during wound healing. J Exp Med 176:1375–1379.

Cha ST, Talavera D, Demir E, Nath AK, Sierra-Honigmann MR. 2005. A method of isolation and culture of microvascular endothelial cells from mouse skin. Microvasc Res 70:198–204.

Dvorak HF, Detmar M, Claffey KP, Nagy JA, van de Water L, Senger DR. 1995. Vascular permeability factor/vascular endothelial growth factor: An important mediator of angiogenesis in malignancy and inflammation. Int Arch Allergy Immunol 107:233–235.

Ferrara N. 2004. Vascular endothelial growth factor: Basic science and clinical progress. Endocr Rev 25:581–611.

Funk CD, Chen XS, Johnson EN, Zhao L. 2002. Lipoxygenase genes and their targeted disruption. Prostaglandins Other Lipid Mediat 68–69:303–312.

Galiano RD, Michaels J, Dobryansky M, Levine JP, Gurtner GC. 2004a. Quantitative and reproducible murine model of excisional wound healing. Wound Repair Regen 12:485–492.

Galiano RD, Tepper OM, Pelo CR, Bhatt KA, Callaghan M, Bastidas N, Bunting S, Steinmetz HG, Gurtner GC. 2004b. Topical vascular endothelial growth factor accelerates diabetic wound healing through increased angiogenesis and by mobilizing and recruiting bone marrow-derived cells. Am J Pathol 164:1935–1947.

Gee E, Milkiewicz M, Haas TL. 2010. p38 MAPK activity is stimulated by vascular endothelial growth factor receptor 2 activation and is essential for shear stress-induced angiogenesis. J Cell Physiol 222:120–126.

Hong S, Gronert K, Devchand PR, Moussignac RL, Serhan CN. 2003. Novel docosatrienes and 17S-resolvins generated from docosahexaenoic acid in murine brain, human blood, and glial cells. Autacoids in anti-inflammation. J Biol Chem 278:14677–14687.

Hong S, Lu Y, Yang R, Gotlinger KH, Petasis NA, Serhan CN. 2007. Resolvin D1, protectin D1, and related docosahexaenoic acid-derived products: Analysis via electrospray/low energy tandem mass spectrometry based on spectra and fragmentation mechanisms. J Am Soc Mass Spectrom 18:128–144.

Kim HY, Karanian JW, Shingu T, Salem N, Jr. 1990. Stereochemical analysis of hydroxylated docosahexaenoates produced by human platelets and rat brain homogenate. Prostaglandins 40:473–490.

Li J, Zhang YP, Kirsner RS. 2003. Angiogenesis in wound repair: Angiogenic growth factors and the extracellular matrix. Microsc Res Tech 60:107–114.

Lu Y, Hong S, Yang R, Uddin J, Gotlinger KH, Petasis NA, Serhan CN. 2007. Identification of endogenous resolvin E1 and other lipid mediators derived from eicosapentaenoic acid via electrospray low-energy tandem mass spectrometry: Spectra and fragmentation mechanisms. Rapid Commun Mass Spectrom 21:7–22.

Lu Y, Tian H, Hong S. 2010. Novel 14,21-dihydroxy-docosahexaenoic acids: Structures, formation pathways, and enhancement of wound healing. J Lipid Res 51:923–932.

Molina PE. 2008. Alcohol—Intoxicating roadblocks and bottlenecks in hepatic protein and lipid metabolism. Am J Physiol Endocrinol Metab 295:E1–E2.

Nissen NN, Polverini PJ, Koch AE, Volin MV, Gamelli RL, DiPietro LA. 1998. Vascular endothelial growth factor mediates angiogenic activity during the proliferative phase of wound healing. Am J Pathol 152:1445–1452.

Radek KA, Kovacs EJ, Gallo RL, DiPietro LA. 2008. Acute ethanol exposure disrupts VEGF receptor cell signaling in endothelial cells. Am J Physiol Heart Circ Physiol 295:H174–H184.

Radek KA, Matthies AM, Burns AL, Heinrich SA, Kovacs EJ, Dipietro LA. 2005. Acute ethanol exposure impairs angiogenesis and the proliferative phase of wound healing. Am J Physiol Heart Circ Physiol 289:H1084–H1090.

Radek KA, Ranzer MJ, Dipietro LA. 2009. Brewing complications: The effect of acute ethanol exposure on wound healing. J Leukoc Biol 86:1125–1134.

Rivara FP, Jurkovich GJ, Gurney JG, Seguin D, Fligner CL, Ries R, Raisys VA, Copass M. 1993. The magnitude of acute and chronic alcohol abuse in trauma patients. Arch Surg 128:907–912, discussion 912–913.

Schneider C, Yu Z, Boeglin WE, Zheng Y, Brash AR. 2007. Enantiomeric separation of hydroxy and hydroperoxy eicosanoids by chiral column chromatography. Methods Enzymol 433:145–157.

Sharma GD, He J, Bazan HE. 2003. p38 and ERK1/2 coordinate cellular migration and proliferation in epithelial wound healing: Evidence of cross-talk activation between MAP kinase cascades. J Biol Chem 278:21989–21997.

Shukla SD, Sun GY, Gibson Wood W, Savolainen MJ, Alling C, Hoek JB. 2001. Ethanol and lipid metabolic signaling. Alcohol Clin Exp Res 25:33S–39S.

Shweiki D, Itin A, Soffer D, Keshet E. 1992. Vascular endothelial growth factor induced by hypoxia may mediate hypoxia-initiated angiogenesis. Nature 359:843–845.

Siebert M, Krieg P, Lehmann WD, Marks F, Furstenberger G. 2001. Enzymic characterization of epidermis-derived 12-lipoxygenase isoenzymes. Biochem J 355:97–104.

Sommers MS. 1994. Alcohol and trauma: The critical link. Crit Care Nurse 14:82–86; 88–93.

Sozio M, Crabb DW. 2008. Alcohol and lipid metabolism. Am J Physiol Endocrinol Metab 295:E10–E16.

Tian H, Lu Y, Sherwood AM, Hongqian D, Hong S. 2009. Resolvins E1 and D1 in choroid-retinal endothelial cells and leukocytes: Biosynthesis and mechanisms of anti-inflammatory actions. Invest Ophthalmol Vis Sci 50: 3613–3620.

VanRollins M, Baker RC, Sprecher HW, Murphy RC. 1984. Oxidation of docosahexaenoic acid by rat liver microsomes. J Biol Chem 259:5776–5783.

Velazquez OC. 2007. Angiogenesis and vasculogenesis: Inducing the growth of new blood vessels and wound healing by stimulation of bone marrow-derived progenitor cell mobilization and homing. J Vasc Surg 45(Suppl A): A39–A47.

Wu Y, Chen L, Scott PG, Tredget EE. 2007. Mesenchymal stem cells enhance wound healing through differentiation and angiogenesis. Stem Cells 25: 2648–2659.